Available online at www.sciencedirect.com
ScienceDirect
Journal of Hazardous Materials 156 (2008) 194–200
Journal of Hazardous Materials
www.elsevier.com/locate/jhazmat

Photocatalytic degradation of organic dyes with manganese-doped ZnO nanoparticles

Ruh Ullah [a,*], Joydeep Dutta [b]

[a] NUST Institute of Information Technology (NIIT), National University of Science and Technology (NUST) Pakistan, 166A, Street 9 Chaklala Scheme III, Tamiz ud din Road, Rawalpindi, Pakistan
[b] Centre of Excellence in Nanotechnology (CoEN), Asian Institute of Technology, P.O. Box 4, Klongluang Pathumthani 12120, Thailand

Received 20 August 2007; received in revised form 10 November 2007; accepted 6 December 2007
Available online 23 December 2007

Abstract

Manganese-doped and undoped ZnO photocatalysts were synthesized via wet-chemical techniques. Doping of ZnO with manganese (Mn^{2+}) was intended to create tail states within the band gap of ZnO. These can subsequently be used as efficient photocatalysts which can effectively degrade organic contaminants only with visible light irradiation. Photocatalysts prepared with these techniques, which were characterized with transmission electron microscopy (TEM), infrared spectroscopy (FTIR), photo-co-relation spectroscopy (PCS) and UV–vis-spectroscopy showed significant difference in the optical absorption of Mn-doped ZnO. Enhancement in optical absorption of Mn-doped ZnO indicates that it can be used as an efficient photocatalyst under visible light irradiation. The photo-reduction activities of photocatalysts were evaluated using a basic aniline dye, methylene blue (MB) as organic contaminant irradiated only with visible light from tungsten bulb. It was found that manganese-doped ZnO (ZnO:Mn^{2+}) bleaches MB much faster than undoped ZnO upon its exposure to the visible light. The experiment demonstrated that the photo-degradation efficiency of ZnO:Mn^{2+} was significantly higher than that of undoped ZnO and might also be better than the conventional metal oxide semiconductor such as TiO_2 using MB as a contaminant.

Keywords: Visible light; Photocatalysis; Mn-doped ZnO nanoparticles

1. Introduction

Since the decomposition of water into hydrogen and oxygen on titanium electrode by Fujishima and Honda in 1972 photocatalysis has been established as an efficient process for the mineralization of toxic organic compounds, hazardous inorganic constituents [1] and bacteria disinfection [2] owing to the strong oxidizing agent, i.e., hydroxyl radical ($OH^{\bullet}$) [3]. Some metal oxide semiconductors like titanium dioxide (TiO_2), zinc oxide (ZnO), tungsten oxide (WO_3), strontium titanate ($SrTiO_3$), and hematite (α-Fe_2O_3) are proven to be dynamic photocatalysts [4]. Most of these semiconductor photocatalysts have band gap in the ultraviolet (UV) region, i.e., equivalent to or larger than 3.2 ev ($\lambda = 387$ nm). Therefore, they promote photocatalysis upon illumination with UV radiation. Unfortunately solar spectrum consists only 5–7% of UV light, while 46% and 47% of the spectrum has visible light and infrared radiation, respectively [5]. This minimal extent of UV light in the solar spectrum has particularly ruled out the use of natural source of light for photocatalytic decomposition of organic and inorganic contaminants and bacteria disinfection from water and air on large scale. Surface and volumetric charge recombination is an additional obstacle that hinders heterogeneous photocatalysis to be an efficient purification method.

Till now anatase form of TiO_2 has been extensively investigated in the field of photocatalysis owing to its complementary physiochemical properties [6]. In order to shift the optical absorption of TiO_2 to the visible region of solar spectrum and circumvent charge recombination on photocatalysts surface, various attempts have been made, such as coupling of TiO_2 with gold and SnO_2 with silver [7]. However, this scheme was unsuccessful to increase photocatalytic activities in the visible

* Corresponding author. Tel.: +92 519280155x140; fax: +92 519280782.
E-mail addresses: ruhullahg@gmail.com, ruhullah@niit.edu.pk (R. Ullah), joy@ait.ac.th (J. Dutta).
URLs: www.niit.edu.pk/~ruhullah (R. Ullah), http://www.nano.ait.ac.th (J. Dutta).

0304-3894/$ – see front matter © 2007 Elsevier B.V. All rights reserved.
doi:10.1016/j.jhazmat.2007.12.033

region. A number of research groups have since approached this issue by doping TiO_2 with different transition metal ions in an effort to lower the transition energy. Fe(III) doping of TiO_2 was reported to have small effect on the efficiency, while Cr(III) doping has shown reduced photo-reactivity for water cleavage and N_2 reduction. TiO_2 was doped with vanadium and utilized for photo-oxidation of 4-chlorophenol (4-CP), but the results reflect that the quantum efficiency of undoped TiO_2 was higher than that of the vanadium-doped TiO_2 [8]. The reduction in quantum efficiency of V-doped TiO_2 was reasoned for the phase transformation of TiO_2 from anatase to rutile at higher temperatures. Chio et al. [9] found that doping of TiO_2 with Fe^{3+}, Mo^{5+}, Ru^{3+}, Os^{3+}, Re^{5+}, V^{4+}, and Rh^{3+} leads to increase photo-reactivity in the liquid-phase photo-degradation of chloroform ($CHCl_3$), whereas doping with Co^{3+} and Al^{3+} has inverse effect on the photo-reactivity of TiO_2. In a recent study by Klosek and Raftery [10] vanadium-doped TiO_2 has been employed for photo-oxidation of ethanol that showed better photo-reactivity but the by-products were carbon monoxide and formic acid which are also hazardous. All these unsuccessful efforts of doping and coupling of TiO_2 to tune its band gap for photocatalysis under visible light illumination motivated us to dope ZnO with metal and transition metals for the reduction of organic compounds under visible light.

ZnO has emerged to be more efficient catalyst as far as water detoxification is concerned because it generates H_2O_2 more efficiently [11], it has high reaction and mineralization rates [12]. Also it has more numbers of active sites with high surface reactivity [13]. ZnO has been demonstrated as an improved photocatalyst as compared to commercialized TiO_2 based on the larger initial rates of activities [14] and its absorption efficacy of solar radiations [15]. However, ZnO has almost the same band gap (3.2 ev) as TiO_2. Surface area and surface defects play an important role in the photocatalytic activities of metal oxide. The reason is that, doping of metal oxide with metal and/or transition metals increases the surface defects [16]. In addition it affects the optical and electronic properties [17] and can presumably shifts the optical absorption towards the visible region. This can subsequently activate these modified metal oxide photocatalysts upon visible light irradiation. Doping of ZnO with cobalt (Co) has been reported [18] to cause hyperchromic shift in the optical absorption of ZnO, which is attributable to the shrinkage of the band gap. These changes in ZnO caused by Co ion were assumed to play an important role in the photocatalysis. As reported ZnO is better solar photocatalyst than TiO_2 and other metal oxide on the basis of solar radiation absorption [15]. In addition enhancement in the optical absorption owing to increase in surface defects by doping with Pb ion [17] and Ag ion [16] urge us to further investigate undoped and doped ZnO nanoparticles and its photocatalytic activities. To improve the photocatalytic activities we doped ZnO with manganese ion (Mn^{2+}) and carried out studies on photocatalytic activities of Mn-doped ZnO using only visible light as source of radiation and methylene blue as test contaminant. The preliminary results presented in this work show much promise and suggest the need to further explore heterogeneous photocatalysis.

2. Experimental

2.1. Preparation of undoped ZnO and Mn-doped ZnO ($ZnO:Mn^{2+}$)

Colloidal solution of undoped ZnO was prepared based on the method described by Hossain et al. [19] and the same techniques were also used with a little modification for Mn-doped ZnO. In a typical synthesis 4 mmol of Zinc acetate were dissolved in 40 ml of ethanol and heated at 50 °C along with vigorous stirring for half an hour, thus making precursor solution A. Then 4 mmol of sodium hydroxide were dissolved in 40 ml of ethanol and heated at 50 °C along with vigorous stirring for 1 h, making precursor solution B. Further more, 0.02 mmol of manganese acetate (dopant) were dissolved in 20 ml of ethanol at 50 °C along with vigorous stirring for half an hour, thus making precursor solution C.

In order to make ZnO-doped/undoped colloids, 20 ml of precursor solution A was complexed with 20 ml of precursor solution C/20 ml of pure ethanol (to keep the concentration of zinc acetate identical in both doped and undoped synthesis process). Both the solutions were heated at 80 °C for another half an hour. After cooling at room temperature, 20 ml of precursor solution B was mixed in each of above solutions for hydrolysis in order to transform zinc hydroxide to ZnO. Both the solutions were kept in water bath at 60–65 °C for 2 h. It was observed that solutions started precipitating after 1 h in water bath. After cooling to room temperature for 4 h, both the colloidal solutions were centrifuged for 20 min at 4000 rpm. Centrifugation was performed to remove the large sized agglomerates so that only nanoparticles of almost uniform size were suspended in the solution. The nanoparticles thus synthesized were then used for further experimental exploration, i.e., photocatalysis.

2.2. Assessment of the photocatalytic activities of undoped and Mn-doped ZnO nanoparticles

Methylene blue solution was prepared by dissolving 1 μmol (one micro mole) of methylene blue ($C_{16}H_{18}ClN_3S$) in 20 ml ethanol. This solution was then used as a test contaminant for investigating photocatalytic activities of the synthesized ZnO and $ZnO:Mn^{2+}$ nanoparticles. The evaluation was carried out both under ultraviolet light and visible light in order to investigate the efficiency of doped ZnO nanoparticles. To examine photocatalytic activity of doped and undoped ZnO nanoparticles 2 ml of colloidal solution (each doped and undoped) and 2 ml of pure ethanol were mixed with 200 μl (micro liter) of MB solution, separately in plastic cuvettes. Three samples, $ZnO:Mn^{2+}$, ZnO and pure ethanol, each mixed with 200 μl MB, were prepared and exposed to visible light. Three similar samples were exposed to UV irradiation (black light) using quartz cuvettes. Visible light from a 500 W tungsten lamp was incident on the samples, where a water tank (one foot high and one foot wide) was placed between the light source and the samples in order to absorb all the infrared and UV radiation originating from the light source. Since light intensity is of immense importance for photocatalytic processes, it was kept constant at 18.6 klux (mea-

sured with light meter from LUTRON, version YK-2001LX) through out the experimental work from the same source of light, i.e., tungsten lamp.

2.3. Characterization of manganese-doped ZnO ($ZnO:Mn^{2+}$) nanoparticles

The optical absorption, crystal structure, and sizes of particles were examined with UV–vis spectrophotometer, TEM, and PCS. Optical characteristics of Mn-doped ($ZnO:Mn^{2+}$) and undoped ZnO were determined with double beam UV–vis spectrophotometer (Model SL 164 from ELICO). Structural characterizations were carried out with transmission electron microscope (JEOL/JEM-2100F version) operated at 200 kV, Fourier transform infrared spectroscope with System 2000FTIR, Perkin Elmer. We used photo-co-relation spectroscopy (PCS) machine from MALVERN Instrument Zetasizer Nano Model ZS Zen3600 fitted with a red laser (633 nm), as it can measure particle size within a range of 0.6–600 nm. Folded capillary cell (DTS1060) was used for zeta potential measurements, and disposable low volume polystyrene (DST0112) cuvette was used for size measurement.

3. Results and discussions

3.1. The size and optical absorption of $ZnO:Mn^{2+}$ nanocrystallites

Synthesis of metal oxide nanoparticles through wet-chemical and co-precipitation techniques involve the dissolution of metal salt, i.e., zinc acetate (in our case) to give zinc ion (Zn^{2+}) and acetate ion (CH_3CHOO^-). Similarly, dissolving manganese acetate gives the corresponding cations and anions. The synthesis of electrostatically stable ZnO nanoparticles is usually performed in alcoholic solution to avoid formation of ZnOH [20]. We therefore made a complex of zinc acetate solution and dopant solution in ethanol. Fourier transform infrared spectroscopy of the hydrolyzed particles (Fig. 1) show strong peaks

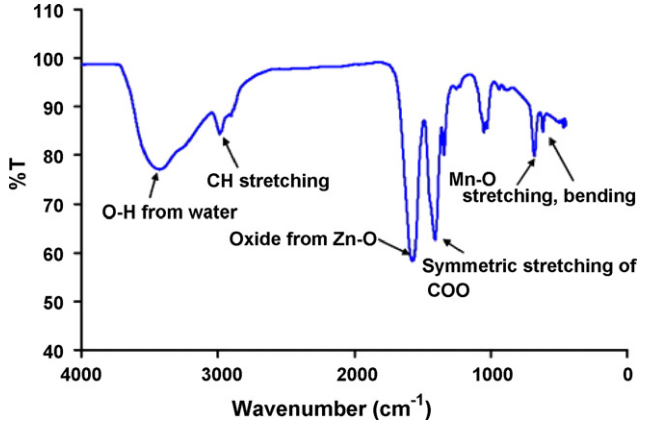

Fig. 1. FTIR-spectroscopy of zinc acetate complexed with manganese acetate in ethanol, peaks at 1404 cm^{-1} corresponds to ZnO and peaks at 674 cm^{-1} and 615 cm^{-1} corresponds to Mn–O stretching and bending while peaks at 3420 cm^{-1} arises from water not from ZnOH.

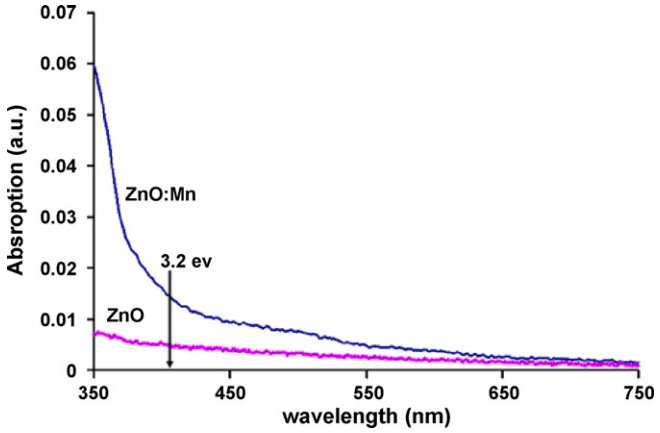

Fig. 2. UV–vis absorption of ZnO, $ZnO:Mn^{2+}$, represents difference in the optical absorption of Mn-doped and undoped ZnO, which indicate that Mn ion can generate more active site for reaction at energy level lower than the conduction band of undoped ZnO and thus absorbs visible light via these defect sites causing enhancement in the optical absorption of ZnO.

at 1562 cm^{-1} and at 1404 cm^{-1}. The former peak at 1562 cm^{-1} indicates the formation of ZnO [21]. Peaks at 674 cm^{-1} and 614 cm^{-1} [22] correspond to Mn–O stretching and bending. These peaks confirm integration of manganese (Mn) ion with zinc (Zn) ion. UV–vis-spectroscopy of both the undoped and Mn-doped ZnO nanoparticles showed evidence of a significant divergence in the absorption intensity at the blue region, as shown in Fig. 2. This huge difference in the optical absorption of ZnO and $ZnO:Mn^{2+}$ demonstrates that manganese-doped ZnO ($ZnO:Mn^{2+}$) absorbs more visible light and therefore can be used as an efficient photocatalyst under visible light irradiation. Copper ion-doped and aluminum ion-doped ZnO were also prepared with similar techniques as described for Mn-doped ZnO. The UV–vis-spectroscopy of all the samples (figure is not shown) suggested that Mn-doped ZnO absorbs more visible light than copper-doped and aluminium-doped ZnO and therefore, was selected for further experimental exploration. This increase in the absorption intensity in the blue region can be attributed to the more pronounced doping of ZnO with manganese ion [23]. It demonstrates that manganese doping in ZnO creates more defect sites as compared to Cu doping [24]. We assumed that the enhancement in the optical absorption of $ZnO:Mn^{2+}$ is due to the increase of defect sites in the crystal structure of the doped ZnO when compared to the undoped ZnO, as illustrated [16,17] in the case of metal ion-doped ZnO. In our case the optimum dopant (Mn) concentration was found to be 1%. This is because reduction in the optical absorption was observed upon further increase in the dopant concentration. This may be attributed to the structural changes of ZnO owing to Mn^{2+} doping [25]. However, we assume that at high dopant concentration Mn^{2+} may react more readily with oxygen to form MnO_x instead of taking interstitial or substitutional site in ZnO crystal.

Doping of ZnO with Mn^{2+} adds tail states in the vicinity of the valence band owing to the defect sites and reduces its effective band gap. This decrease in the band gap [26], which subsequently causes red shift in the optical absorption of Mn^{2+}-doped ZnO nano\microfilms [27] and nanoparticles [28] has

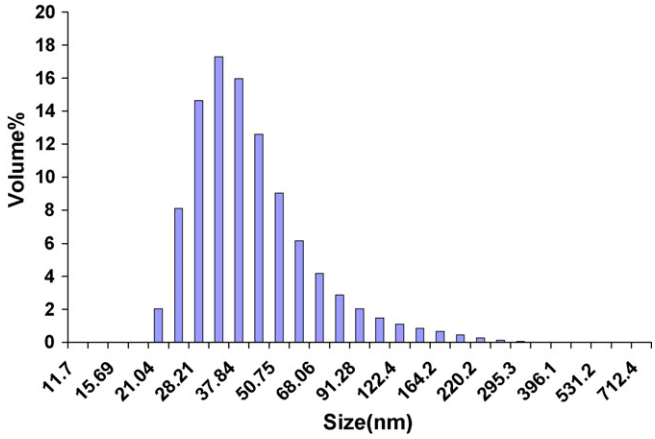

Fig. 3. Statistical volume % distribution of ZnO:Mn^{2+} illustrating average particle size of almost the same as SEM analysis.

been reported for lower dopant concentration. Upon irradiation with UV–vis light electron–hole pair is generated within the effective band gap, i.e., electron transition takes place from the defect valence state to the defect conduction state. This transition within the tail states requires smaller excitation energy as compared to the native band gap (3.2 ev) of ZnO depending upon the particular dopant level within the band gap.

Particle size and surface area have key effects on the photocatalytic activities of photocatalyst. Thus photo-correlation spectroscopy was performed to measure the average particle size and zeta potential of colloids. The average particle size so obtained was 73 nm while particle having average size of 37.84 nm has the highest volume % as shown in Fig. 3 that has also been estimated from TEM micrograph. Photocatalysts need to be stable, while ZnO is also relatively stable and is resistant to electrochemical corrosion when used as photocathode [29]. Zeta potential of doped colloids was measured to be −23.4 mV, which indicates relative stability of the colloids. Electrostatic stability of colloidal suspension arises from the electrical double layer in the vicinity of particle [30]. Thus ZnO:Mn^{2+} nanoparticles have OH^- on their surface which make the surface negatively charged. Thus Na ion (Na^+) existing in the solution makes an other layer around the particle and hence creating electrical double layer around ZnO:Mn^{2+}. This electrical double layer is responsible for particle stability. TEM analysis of the ZnO and ZnO:Mn^{2+} particles was performed after drying the samples on TEM grid for more than 12 h. The TEM micrographs showed crystalline size of 3–5 nm, agglomerated into polycrystalline structures of different sizes ranging from 21 nm to 73 nm on average as shown in Fig. 4. Crystallographic planes (shown in Fig. 5) of ZnO and ZnO:Mn^{2+} were determined applying fast Fourier transform (FFT) and inverse FFT analysis to the transmission electron micrograph. The imaged lattice spacing amounts to 1.6 Å and 1.9 Å corresponding to (1 1 0) and (1 0 2) planes confirming the wurtzite structure of ZnO [31,32] nanocrystallites.

3.2. Evaluation of the photocatalytic activities of ZnO and ZnO:Mn^{2+} nanoparticles

The photocatalytic activities of undoped ZnO and ZnO:Mn^{2+} were carried out using UV light and visible light. MB was used as a test contaminant since it has been extensively used as an indicator for the photocatalytic activities [16,33] owing to its absorption peaks in the visible range. Hence its degradation can be easily monitored by optical absorption spectroscopy. Furthermore, a large portion of water-borne pollutants is known to be from synthetic textile dye and industrial dyes stuffs. First photodegradation of methylene blue (MB) was carried with ZnO and ZnO:Mn^{2+} by irradiating mixture of photocatalyst and MB with ultraviolet light (UV). It was observed that undoped ZnO decolorizes MB faster than doped ZnO. It was also observed that about 50% of MB degraded within 10 min by ZnO while it took 30 min for ZnO:Mn^{2+} to bleach the same quantity of MB as used for undoped nanoparticles (shown in Figs. 6 and 7, respectively). Photocatalytic activity of undoped ZnO is attributed both to the donor states caused by the large number of defect sites such as oxygen vacancies and interstitial zinc atom and to the acceptor states which arise from zinc vacancies and interstitial oxy-

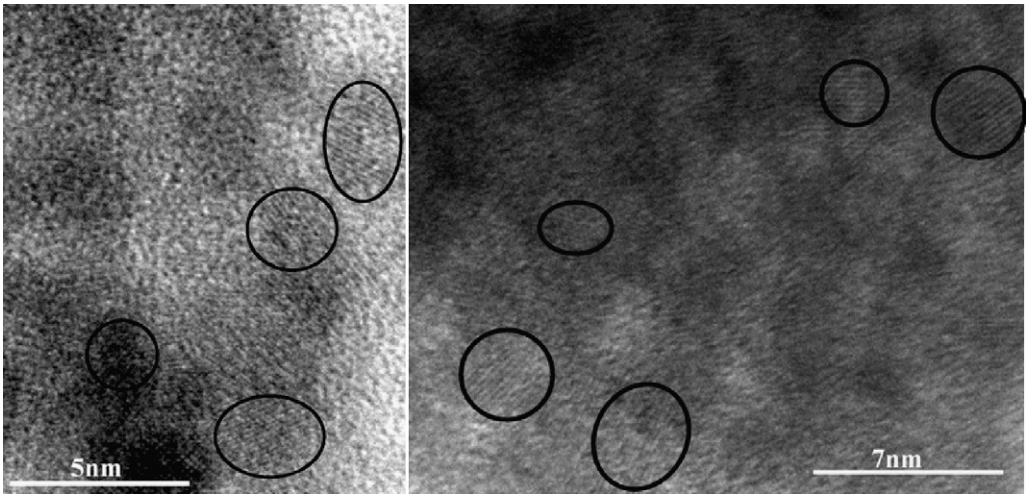

Fig. 4. TEM micrograph of ZnO, ZnO:Mn^{2+} reveals polycrystalline structure with average crystal size of about 3–5 nm.

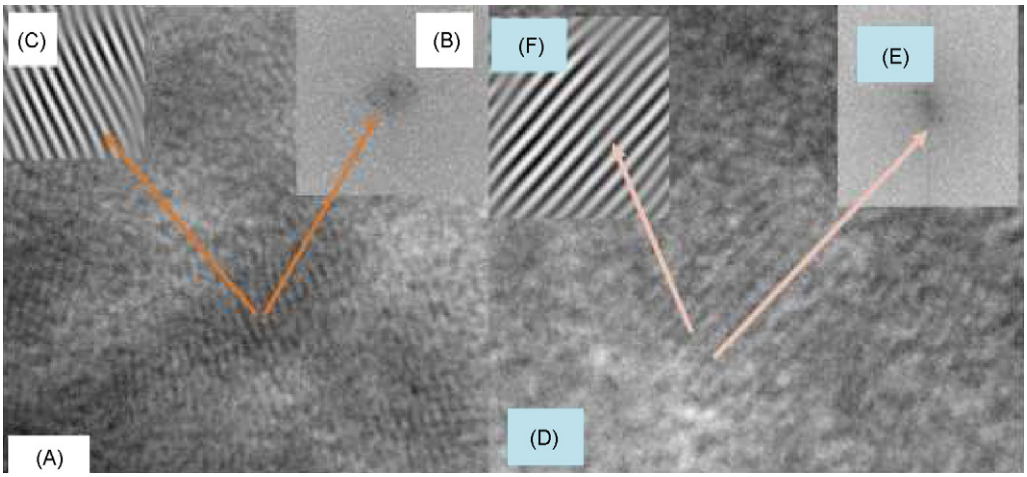

Fig. 5. TEM micrograph of ZnO (A)and ZnO:Mn^{2+}(D) and the corresponding FFT and inverse FFT. The inset at the right top (B, E) is the processed FFT of the TEM images and the left top of the images (C, F) are corresponding crystallographic planes obtained from reverse FFT of inset B and E, respectively.

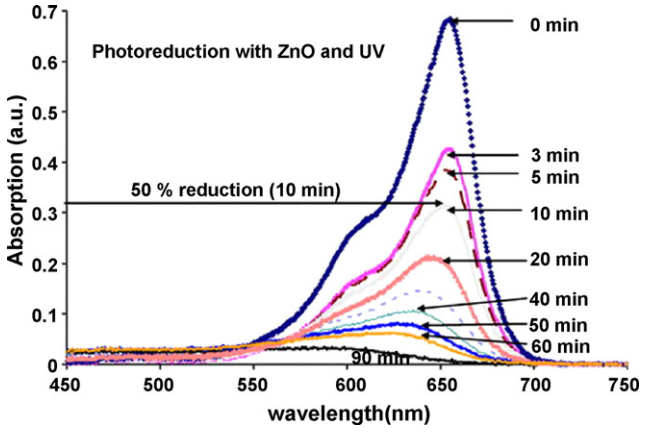

Fig. 6. Photo-reduction of MB with ZnO and UV light.

gen atoms [34]. Oxygen vacancies located at energy positions 2.35–2.50 eV is responsible for green luminescence upon illumination with UV light. Here we assume that interfacial electron transfer takes place predominantly between these donor states (oxygen vacancies and interstitial Zn atom) and MB instead of radiative charge recombination which causes green emission in ZnO. Being a cationic dye MB acquires electron from excited donor states and decomposes. Lower photo-degradation of MB with UV and doped ZnO (ZnO:Mn^{2+}) may be attributed to the change in absorption characteristics caused by Mn^{2+} doping. We assume that this lower photo-degradation maybe due to the faster recombination of electron–hole pair [35]. Degradation of MB was also examined using ZnO and ZnO:Mn^{2+} without light irradiation. Samples were kept in dark for more than 6 h but there was no degradation at all as shown in Fig. 10 (topmost curve). Only methylene blue dissolved in water shows very small degradation (second curve in Fig. 10) when irradiated with visible light. This smaller degradation of MB might be due to the interaction of MB with $OH^{\bullet}$ radical originated from water [36]. We assume that unlike water, irradiation of ethanol with visible light may not lead to the generation of hydroxyl radical, which could subsequently degrade MB. Therefore, no degradation of MB was observed when mixed with ethanol and exposed to visible light (as shown in the topmost curve of Fig. 10).

Photo-degradation rate of MB with ZnO:Mn^{2+} irradiated with visible light was much faster than with ZnO irradiated with visible light and ZnO irradiated with UV light as shown in

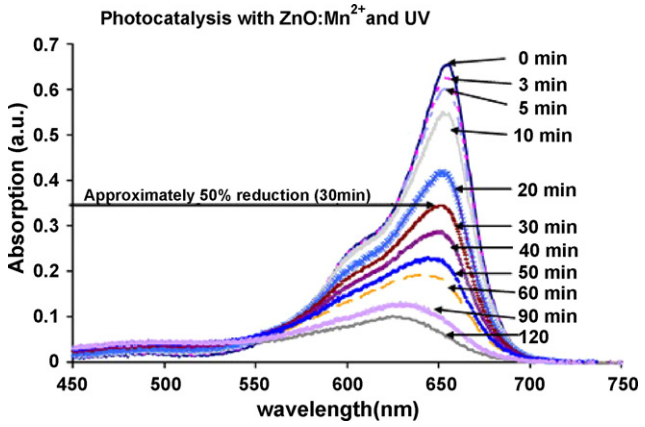

Fig. 7. Photo-reduction of MB using ZnO:Mn^{2+} and UV light.

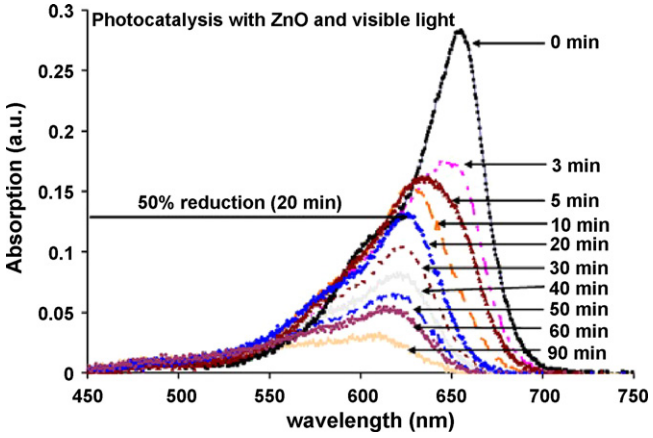

Fig. 8. Photo-reduction of MB with ZnO and visible light.

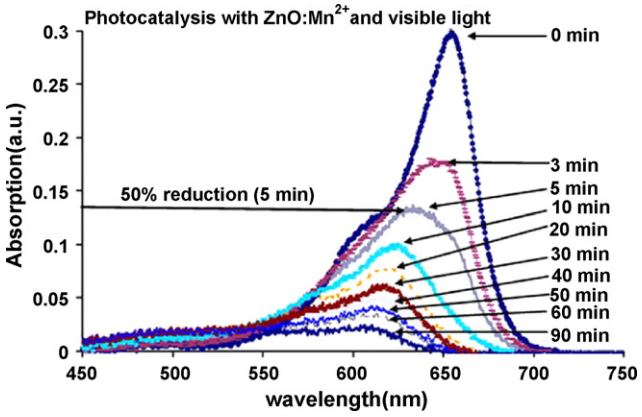

Fig. 9. Photo-reduction of MB with ZnO:Mn^{2+} and visible light.

Figs. 8 and 9, respectively. It took only 5 min for ZnO:Mn^{2+} to decolorize 50% of MB while for ZnO it took more than 20 min to decolorize the similar amount of MB. This faster degradation rate of MB under visible light irradiation using ZnO:Mn^{2+} is attributed to the increase in defect sites caused by Mn^{2+} doping, leading to an enhanced optical absorption in the visible region. Comparison of the photo-reduction rate of MB with ZnO:Mn^{2+}/visible light, ZnO:Mn^{2+}/UV light, ZnO/visible light, ZnO/UV light, and ZnO:Mn^{2+}, ZnO kept in dark is shown in Fig. 10. This clearly demonstrates that ZnO doped with Mn^{2+} (ZnO:Mn^{2+}) degrades MB more efficiently than undoped ZnO. It is evident that doping of ZnO with transition metals like Mn enhances photocatalytic activities of ZnO, and hence ZnO:Mn^{2+} is capable of degrading MB and other organic dyes even with

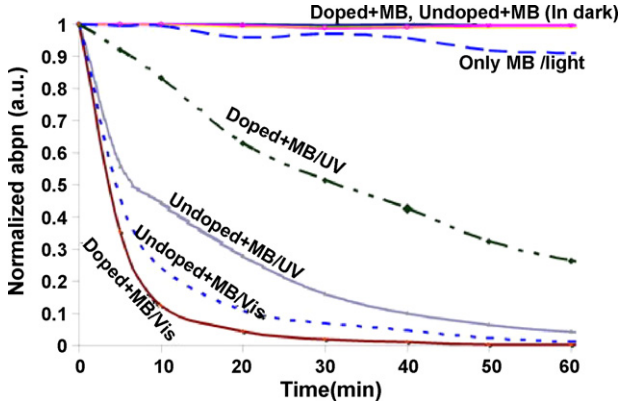

Fig. 10. Photo-reduction of MB with respect to time using doped and undoped ZnO exposed to UV light, visible light and kept in dark. Only MB (without photocatalysts) exposed to UV light, visible light and kept in dark. The topmost curve represents ZnO doped and undoped mixed with MB and only MB mixed in pure ethanol/water kept for more than 6 h in dark, which did not show degradation of MB in the absence of light. Second curve correspond to MB dissolved in water and expose to light which shows a slight degradation, because of OH^- in water. Third curve corresponds to MB mixed with ZnO:Mn^{2+} and was exposed to UV, while the fourth curve from undoped ZnO mixed with MB and exposed to UV illustrate that, undoped ZnO has better photo-degradation response than doped ZnO using UV light. Curves fifth and sixth are from undoped ZnO and ZnO:Mn^{2+} mixed with MB and exposed to only visible light, which clearly indicates the effect of Mn doping on ZnO photocatalytic activity, i.e., on photo-degradation of MB.

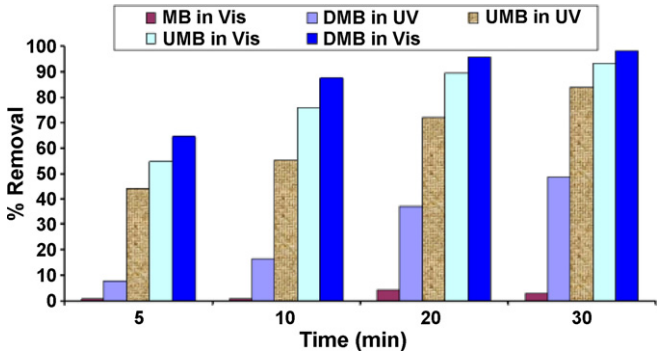

Fig. 11. Percentage photo-reduction of MB using ZnO, ZnO:Mn^{2+},UV light, and visible light, where the right most one within each group is the percentage removal of MB with visible light and ZnO:Mn^{2+}. MB in vis: only methylene blue irradiated with visible light; DMB in UV: doped ZnO (ZnO:Mn^{2+}) and methylene blue irradiated with UV light; UMB in UV: undoped and methylene blue irradiated with UV light; UMB in vis: undoped ZnO and methylene blue irradiated with visible light; DMB in vis: doped ZnO (ZnO:Mn^{2+}) and methylene blue irradiated with visible light.

the visible light irradiation. Here, we assumed that upon illumination with visible light, ZnO:Mn^{2+} generates electron–hole pair at the tail states of conduction band and valence band, respectively. The generated electron transfers to the adsorbed MB molecule on the particle surface because it is a cationic dye. The excited electron from the photocatalyst conduction band enters into the molecular structure of MB and disrupts its conjugated system which then leads to the complete decomposition of MB. Hole at the valence band generates $OH^{\bullet}$ via reaction with water or OH^-, might be used for oxidation of other organic compounds. Percentage photo-reduction of MB using doped and undoped ZnO irradiated with UV and visible light is also shown in Fig. 11. This clearly demonstrates that ZnO doped with manganese (ZnO:Mn^{2+}) can be used as a potential photocatalyst, which can operate at visible light.

4. Conclusion

From literature it is well known that ZnO is a wide and a direct band gap material that has been shown to demonstrate photocatalytic activities. We therefore, synthesized Mn-doped ZnO nanocrystals for the first time using wet-chemical precipitation techniques. The newly synthesized ZnO:Mn^{2+} has been observed as an excellent photocatalyst under visible illumination. ZnO:Mn^{2+} photocatalysts showed promising results for degradation of organic dye with visible light irradiation when used as suspended colloids. From the results we conclude that the photocatalytic activities of doped ZnO nanoparticles are close to 50 times higher than ZnO under visible light irradiation. These preliminary results suggest that ZnO:Mn^{2+} nanoparticles can be used as immobilized photocatalysts for water and environmental detoxification from organic compounds, inorganic compounds like arsenic and bacteria. The development of such photocatalysts may be considered a breakthrough in large-scale utilization of heterogeneous photocatalysis via visible light to address water contamination and environmental pollution.

Acknowledgments

The work was performed at the center of excellence in nanotechnology in Asian Institute of Technology (AIT), Thailand. The authors would also like to acknowledge the facilities and help provided by the School of Engineering and Technology of AIT.

References

[1] J.M. Herrmann, Heterogeneous photocatalysis: fundamentals and applications to the removal of various types of aqueous pollutants, J. Catal. Today 53 (1999) 115–129.
[2] P.C. Maness, S. Smolinski, D.M. Blake, Z. Huang, E.J. Wolfrum, W.A. Jacoby, Bactericidal activity of photocatalytic TiO_2 reaction: toward an understanding of its killing mechanism, Appl. Environ. Microbiol. 65 (1999) 4094–4098.
[3] Z. Huang, P.C. Maness, D. Blake, E.J. Wolfrum, S.L. Smolinski, W.A. Jacoby, Bactericidal mode of titanium dioxide photocatalysis? J. Photochem. Photobiol. A 130 (2000) 163–172.
[4] D.S. Bhatkhande, D.S. Pangarkar, A.ACM. Beenackers, Photocatalytic degradation for environmental applications—a review, J. Chem. Technol. 77 (2001) 102–116.
[5] T. Bak, J. Nowotny, M. Rekas, C.C. Sorrell, Photo-electrochemical hydrogen generation from water using solar energy. Materials-related aspects, Int. J. Hydrogen Energy 27 (2002) 1022–27991.
[6] X.Z. Li, F.B. Li, Study of Au/Au^{3+}–TiO_2 photocatalysts toward visible photooxidation for water and wastewater treatment, J. Enivron. Sci. Technol. 35 (2001) 2381–2387.
[7] P.V. Kamat, Photo-induced transformations in semiconductor–metal nanocomposite assemblies, J. Appl. Chem. 74 (2002) 1693–1706.
[8] S.T. Martin, C.L. Morrison, M.R. Hoffmann, Photochemical mechanism of size-quantized vanadium-doped TiO_2 particles, J. Phys. Chem. 98 (1994) 13695–13704.
[9] W. Chio, A. Termin, M.R. Hoffmann, The role of metal ion dopants in quantum-sized TiO_2: correlation between photoreactivity and charge carrier recombination dynamics, J. Phys. Chem. 98 (1994) 13669–13679.
[10] S. Klosek, D. Raftery, Visible light driven V-doped TiO_2 photocatalyst and its photo-oxidation of ethanol, Phys. Chem. B 105 (2001) 2815–2819.
[11] E.R. Carraway, A.J. Hoffman, M. Hoffmann, Environ. Sci. Technol. 28 (1994) 786–793.
[12] I. Poulios, D. Makri, X. Prohaska, Photocatalytic treatment of olive milling waste water, oxidation of protocatechuic acid, global nest, Int. J. 1 (1999) 55–62.
[13] B. Pall, M. Sharon, Enhanced photocatalytic activity of highly porous ZnO thin films prepared by sol–gel process, Mater. Chem. Phys. 76 (2002) 82–87.
[14] K.Y. Jung, Y.C. Kang, S.B. Park, Photodegradation of trichloroethylene using nanometre-sized ZnO particles prepared by spray pyrolysis, J. Mater. Sci. Lett. 16 (1997) 1848–1849.
[15] S. Sakthivel, B. Neppolian, M.V. Shankar, B. Arabindoo, M. Palanichamy, V. Murugesan, Solar Energy Solar Cells 77 (2003) 65–82.
[16] R. Wang, J.H. Xin, Y. Yang, H. Liu, L. Xu, J. Hu, The characteristics and photocatalytic activities of silver-doped ZnO nanocrystallites, Appl. Surf. Sci. 227 (2004) 312–317.
[17] K. Vanhesuden, W.L. Warren, J.A. Voigt, C.H. Seager, D.R. Tallant, Impact of Pb doping on the optical and electronic properties of ZnO powders, Appl. Phys. Lett. 67 (1995) 1280–1282.
[18] S. Colis, H. Bieber, S. Begin-Colin, G. Schmerber, C. Leuvrey, A. Dinia, Magnetic properties of Co-doped ZnO diluted magnetic semiconductors prepared by low-temperature mechanosynthesis, Chem. Phys. Lett. 422 (2006) 529–533.
[19] M.K. Hossain, S.C. Ghosh, Y. Boontongkong, C. Thanachayanont, J. Dutta, Growth of ZnO nanowires and nanobelt for gas sensing application, J. Metastable Nanocryst. Mater. 23 (2005) 27–30.
[20] Z. Hu, J.F.H. Santos, G. Oskam, P.C. Searson, Influence on the reaction concentrations on the synthesis of ZnO nanoparticles, J. Colloid Interface Sci. 288 (2005) 313–316.
[21] G.V. Seguel, B.L. Rivas, C. Novas, Polymeric lingand–metal acetate interactions. Spectroscopic study and semi-empirical calculations, J. Chil. Chem. Soc. 50 (No. 1) (2005).
[22] S.J. Parikh, J. Chorover, FTIR spectroscopic study of biogenic Mn-oxide formation by *Pseudomonas putida* GB-1, Geomicrobiol. J. 22 (2005) 207–218.
[23] F.D. Paraguay, M.M. Yoshida, J. Morales, J. Solis, W.L. Estrada, Influence of Al, In, Cu, Fe and Sn dopants on the response of thin films ZnO gas sensor to ethanol vapour, J. Thin Solid Films 373 (2000) 137–140.
[24] H.T. Cao, Z.L. Pie, J. Gong, C. Sun, R.F. Huang, L.S. Wen, Preparation and characterization of Al and Mn-doped ZnO (ZnO:(Al, Mn)) transparent conducting oxide films, J. Solid State Chem. 177 (2004) 1480–1487.
[25] R. Viswanatha, S. Sapra, S.S. Gupta, B. Satpati, P.V. Satyam, Synthesis and characterization of Mn-doped ZnO nanocrystals, J. Phys. Chem. 108 (2004) 6303–6310.
[26] Z.B. Bahsi, A.Y. Oral, Effects of Mn and Cu doping on the microstructures and optical properties of sol–gel derived ZnO thin films, Opt. Mater. 29 (2007) 672–678.
[27] U.N. Maiti, P.K. Ghosh, S. Nandy, K.K. Chattopadhyay, Effect of Mn doping on the optical and structural properties of ZnO nano/micro-fibrous thin film synthesized by sol–gel technique, Physica B 387 (2007) 103–108.
[28] R. Viswanatha, S. Sapra, S.S. Gupta, B. Satpati, P.V. Satyam, Synthesis and characterization of Mn-doped ZnO nanocrystals, J. Phys. Chem. B 108 (2004) 6303–6310.
[29] T. Bak, J. Nowotny, M. Rekas, C.C. Sorrell, Photo-electrochemical hydrogen generation from water using solar energy, Int. J. Hydrogen Energy 27 (2002) 991–1022.
[30] H.C. Warad, S.C. Ghosh, B. Hemtanon, C. Thanachayanont, J. Dutta, Luminescent nanoparticles of Mn-doped ZnS passivated with sodium hexametaphosphate, Sci. Technol. Adv. Mater. 6 (2005) 296–301.
[31] A. Sugunan, H.C. Warad, M. Boman, J. Dutta, ZnO nanowires in chemical bath on seeded substrates: role of hexamine, J. Sol–gel Sci. Technol. 39 (1) (2006) 49–56.
[32] H. Zhou, H. Alves, D.M. Hofmann, B.K. Meyer, G. Kaczmarczyk, A. Hoffmann, C. Thomsen, Effect of the (OH) surface capping on ZnO quantum dots, Phys. Status Solidi B 229 (2002) 825–828.
[33] H. Lachheb, E. Puzenat, A. Houas, M. Ksibi, E. Elaloui, C. Guillard, J.M. Hermman, Photocatalytic degradation pathway of methylene blue in water, Appl. Catal. B: Environ. 31 (2) (2001) 145–157.
[34] F. Tuomisto, K. Saarinen, Introduction and recovery of point defects in electron-irradiated ZnO, Phys. Rev. 72 (2005) 085206-1–085206-11.
[35] S. Anandan, A. Vinu, K.L.P. Sheeja Lovely, N. Gokulakrishnan, P. Srinivasu, T. Mori, V. Murugesan, V. Sivamurugan, K. Ariga, Photocatalytic activity of La-doped ZnO for the degradation of monocrotophos in aqueous suspension, J. Mol. Catal. A: Chem. 266 (2007) 149–157.
[36] M. Panizz, A. Barbucci, R. Ricotti, G. Cerisola, Electrochemical degradation of methylene blue, Sep. Purif. Technol. 54 (2007) 382–387.